

Preparation and characterization of HTSC $\text{LuBa}_2\text{Cu}_3\text{O}_{6+x}$ single crystals

L.P. Kozeeva, M. Yu. Kameneva, N.V. Podberezskaya, D. Yu. Naumov, N.F. Beizel, U-Hyon Paek^a and V.E. Fedorov*
Institute of Inorganic Chemistry, Siberian Branch of the Russian Academy of Sciences, Acad. Lavrentiev ave. 3, Novosibirsk 630090, Russia

^aDepartment of Chemistry, Gyeongsang National University, Chinju, Gyeongnan 660-701, Korea

For the first time large HTSC (high temperature superconductive) crystals of $\text{LuBa}_2\text{Cu}_3\text{O}_{6+x}$ (up to $5 \times 5 \times 0.2 \text{ mm}^3$) were obtained from the Lu_2O_3 -BaO-CuO system by a flux growth method. The crystals obtained were characterized by differential thermal analysis (DTA), chemical and X-ray diffraction analyses. The temperature of incongruent melting of the phase was defined more exactly ($950 \pm 5^\circ\text{C}$). The composition of crystals corresponds to the formula $\text{LuBa}_2\text{Cu}_3\text{O}_{6+x}$. The crystal structure of the tetragonal form was determined and $x=0$ was found for this case.

Key words: A. Superconductors, B. Crystal growth, C. X-Ray diffraction, D. Crystal structure.

Introduction

After the discovery of superconductivity near 90 K in $\text{YBa}_2\text{Cu}_3\text{O}_{6-x}$ (123-Y) every possible substitution of cations, and first of all, full substitution of Y by different R (R=rare earth elements) was conducted. All compounds 123-R, with the exception of Ce, Pr, and Tb, demonstrate some superconducting properties. This gives grounds for many experimenters to say that the R^{3+} cations play a role in the formation of the structure of 123-R phases [1-3]. However, decreasing the ionic radius of the R^{3+} cations in the row of rare earth elements has an influence not only on the stability of 123-R compounds, the kinetics and mechanism of their formation [1, 4, 5], but also influences their physical properties [6-9]. The substitution of the Y^{3+} cation by Lu^{3+} cation which is the smallest one among the R^{3+} series is of special interest for the study of the influence of ionic radius of R^{3+} on the superconducting properties. However, this compound has been studied least among the HTSC 123-R series. This can be explained by difficulties of synthesis of single-phase ceramic samples of 123-Lu as well as growing crystals of it.

Repeated attempts by different researchers to obtain this compound using solid state synthesis gave only small quantities of the 123-Lu phase along with related compounds [2, 10]. Hodorowicz *et al.* [4] concluded that the 123-Lu phase could not be obtained because of the small size of Lu^{3+} . Other authors [11] think that the lowest limit of the R^{3+} radii, which allows the formation of the 123 phase, is close to Yb^{3+} .

Data on the growth of 123-Lu single crystals are extremely limited also. In references [12-14] some physical properties of 123-Lu single crystals with a size $1.2 \times 0.9 \times 0.07 \text{ mm}^3$ can be found but the conditions for crystal growth were not given. Earlier, we have reported briefly about growing 123-Lu single crystals and their properties [9, 15-17]. In this paper we focus our study on the special features of 123-Lu phase formation in the process of spontaneous crystallization from the nonstoichiometric molten Lu_2O_3 -BaO-CuO system, the optimization of the growth conditions and the refinement of the structure of 123-Lu single crystals.

Experimental

Crystals were grown by spontaneous crystallization from the nonstoichiometric molten Lu_2O_3 -BaO-CuO system. All starting compounds (Lu_2O_3 , BaO_2 or BaCO_3 and CuO) had a purity not less than 99.99%. Al_2O_3 crucibles were used. A crucible with an initial mixture (a total mass is about 50-100 g) was placed into a vertical electrical furnace, the temperature gradient in which was about 2 Kcm^{-1} . The detailed description of the equipment and growth method was published earlier [15, 16]. The cationic composition of the crystals obtained was determined by chemical and microprobe methods. For analysis of Lu, a spectrophotometric method (Arsenaso III, spectrophotometer SF-46) was used. Ba was determined by flame photometry, and Cu - by atomic absorption (air-acetylene flame, Hitachi Z-8000) methods. Al impurity content in crystals was determined by atomic emission spectrometry (PGS-2, Germany). Some other methods for characterization were applied: X-ray powder diffraction (DRON-3, Cu K_α); DTA (TA-7000, Japan, heating rate

*Corresponding author:
Tel : 3832-344253
Fax: 3832-344489
E-mail: fed@che.nslc.se

5 Kminute⁻¹; mass of sample was about 50 mg, Al₂O₃ crucible, ±5°C); scanning electron microscopy (JSM-35, Link). Superconducting properties were determined from electroresistivity data [9]. To change the oxygen contents the crystals were heated in air or an oxygen flow.

Structural refinement was carried out using diffraction data obtained from single crystals. Data were collected by standard techniques at room temperature on an Enraf Nonius CAD-4 diffractometer up to $\theta_{\max}=35^\circ$, using MoK α radiation ($\lambda=0.71069 \text{ \AA}$) and ω - 2θ scan mode. Data were corrected for absorption using the real habit of crystal (face indexes).

Results and Discussion

It is known that in the systems R₂O₃-BaO-CuO the crystallization temperatures of 123-R and BaCuO₂ phases become close in the row of rare earth elements R after Gd [15, 18]. For example, for the system Lu-Ba-Cu-O, the rival crystallization of BaCuO₂ in the concentration field of the crystallization of the 123-Lu phase is a reason for unstable crystal growth for the later phase. Therefore to optimize the growth of 123-Lu single crystals it is necessary to depress the growth of the BaCuO₂ phase using an optimal initial chemical composition and an exact temperature interval determined from the incongruent melting temperature of

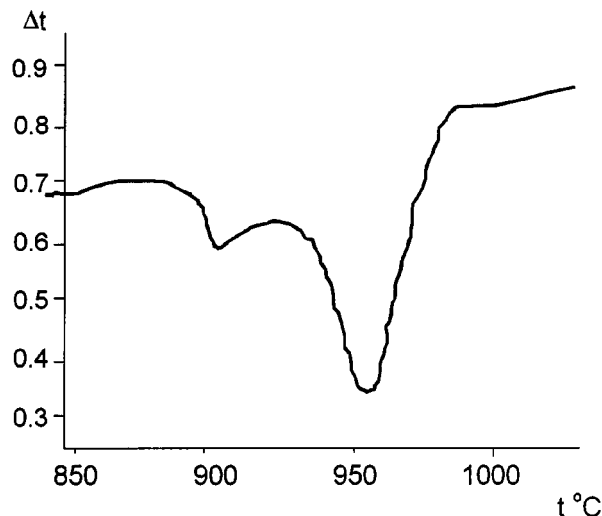


Fig. 1. DTA heating curve of LuBa₂Cu₃O_{6+x}.

123-Lu.

In the existing literature we did not find reliable data on the phase diagram of system the Lu₂O₃-BaOCuO nor the incongruent melting temperature of 123-Lu. It seems that incongruent melting temperatures of 880°C and [8] 870°C [19] are conservative values because of the inhomogeneity of samples studied. Therefore we have determined the melting temperature for three single crystal samples of LuBa₂Cu₃O_{6+x} obtained from

Table 1. Experimental conditions and results of LuBa₂Cu₃O_{6+x} crystal growth

N experiment	Molar ratio Lu ₂ O ₃ :BaO:CuO	123-Lu, mass. %	Isothermal heating		Cooling rate, Khour ⁻¹	Decanting temperature, °C	Phase composition of crystallization products (by visual-microscopic observation)
			T °C	t, hours			
1	0.008:0.287:0.705	10.5	990	10	0.3	900	BaCuO ₂ (5-7 mm) LuBa ₃ Al ₂ O _x
2	-<<	-<<	985	10	0.3	890	123-Lu (1-1.5 mm) BaCuO ₂ up to 5 mm
3	-<<	-<<	980	10	0.5	885	123-Lu (not much) BaCuO ₂ , CuO (1-2 mm, not much)
4	-<<	-<<	985	24	0.5	887	123-Lu up to 2 mm BaCuO ₂ (1-2 mm) CuO (1-2 mm, not much)
5	-<<	-<<	990	24	0.3	885	123-Lu (1-2 mm) BaCuO ₂ (5-7 mm) CuO (1-2 mm, not much)
6	0.014:0.293:0.692	20	1000	25	0.3	885	BaCuO ₂ , CuO, LuBa ₃ Al ₂ O _x
7	0.010:0.290:0.700	15	990	15	0.3	885	BaCuO ₂ up to 5 mm, CuO, LuBa ₃ Al ₂ O _x , Lu ₂ BaCuO ₅ (not much)
8	0.010:0.289:0.701	13.6	1005	20	0.3	887	BaCuO ₂ up to 5 mm, CuO, LuBa ₃ Al ₂ O _x , Lu ₂ BaCuO ₅ (not much)
9	0.009:0.288:0.703	12.8	1005	40	0.3	880	123-Lu up to 2-3 mm and one large crystal 6×7×0.3 mm, BaCuO ₂ up to 2 mm, CuO up to 2 mm, LuBa ₃ Al ₂ O _x
10	-<<	-<<	1010	45	0.3	885	123-Lu up to 3 mm (large yield) BaCuO ₂ up to 2 mm (not much) CuO, LuBa ₃ Al ₂ O _x
11	-<<	-<<	1005	25	0.3	Without decanting	123-Lu (3-4 mm), large blocks BaCuO ₂ , CuO

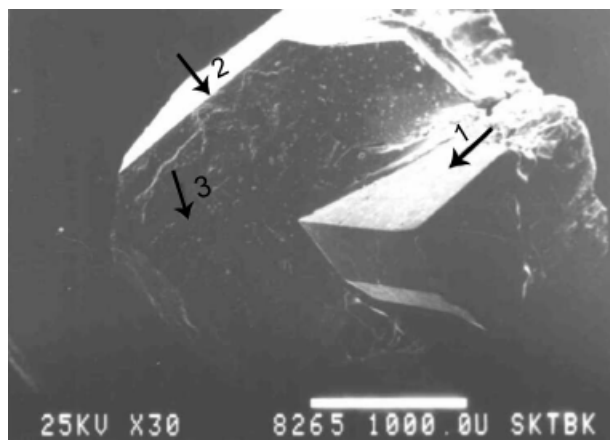


Fig. 2. Micrograph reflecting the result of competitive processes of crystallization of 123-Lu and BaCuO_2 .

different experiments using the DTA method. These samples were practically single phase ones with only very small quantities of impurities (traces of CuO and BaCuO_2). Fig. 1 shows a heating curve of 123-Lu, which is similar to other 123-R phases [19-21]. There are two endothermic effects: a small peak at $910 \pm 5^\circ\text{C}$ which is often attributed to melting of the ternary eutectic [22] and a large peak at $950 \pm 5^\circ\text{C}$ which corresponds to incongruent melting of $\text{LuBa}_2\text{Cu}_3\text{O}_{6+x}$.

The results of crystal growth in the system Lu_2O_3 - BaO - CuO are presented in Table 1. During the process two types of crystals, namely BaCuO_2 and 123-Lu, are usually formed and sometimes these crystals are joined. In some experiments additional phases (CuO , BaAl_2O_4 , $\text{LuBa}_3\text{Al}_2\text{O}_x$) are observed. The size of crystals of 123-Lu can run up to 5-7 mm. Figure 2 demonstrates the result of the competitive processes of crystallization of 123-Lu and BaCuO_2 : a crystal BaCuO_2 (shown by arrow 2) is growing on a crystal 123-Lu (arrow 1) which was formed in the first stage; in the final stage thin films of 123-Lu (shown by arrow 3) begin to grow again. The phases were identified by morphological features as well as by using a microprobe method.

The best results on crystal preparation were obtained using the following experimental conditions: starting composition (Lu_2O_3 : BaCO_3 : CuO = 0.009:0.288:0.703) was heated up to 1010°C , kept at this temperature ≥ 25 hours and then cooled with rate of 0.3 K/hour to 880 - 885°C . At this temperature the crystals were separated from the liquid phase by decanting. This procedure allowed us to obtain a repeatability of experiments and to increase the yield of crystals of 123-Lu, although BaCuO_2 was the main attendant phase in the final products. The crystals obtained were of plate form (Fig. 3) with mean sizes about $3 \times 3 \times 0.2 \text{ mm}^3$, although some of them run up to 5-7 mm.

Chemical analyses of the crystals give a composition $\text{Lu}_{0.99}\text{Ba}_{1.92}\text{Cu}_3\text{O}_{6+x}$. The cation ratio Lu:Ba:Cu is also equal to 1:2:3 from microprobe analyses data (Fig. 4a). The homogeneity of the cationic composition along a

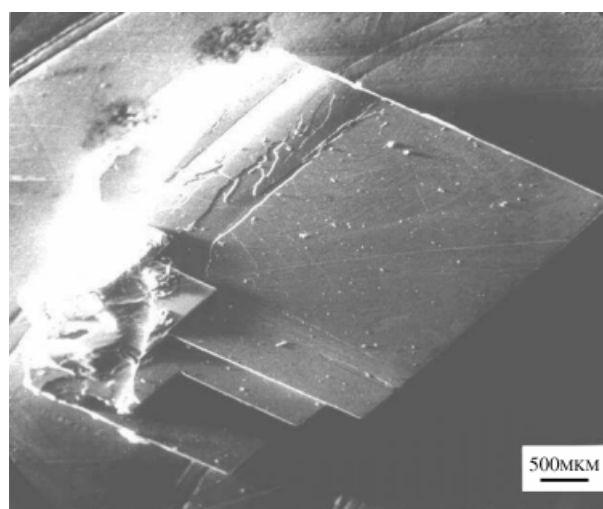
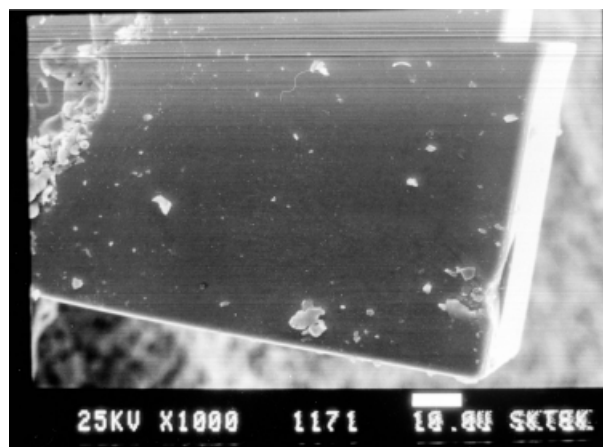


Fig. 3. Grown crystals of $\text{LuBa}_2\text{Cu}_3\text{O}_{6+x}$.

crystal and its repeatability for different crystals are rather high (Fig. 4b). The content of the Al impurity in 123-Lu crystals, which comes through interaction of the reaction melt with the Al_2O_3 crucible, did not exceed 0.2%. The small Al content in crystals is rather a positive fact, since high Al contents are a remarkable feature of 123-R crystals for Tm and Lu (the end rare earth elements). This can be explained by a lower crystallization temperature of 123-R (R=Tm, Lu), as well as preferable participation of Al^{3+} in the formation of secondary phases, in particular $\text{RAl}_3\text{Al}_2\text{O}_x$, that always exists in visible quantities in the Tm- and Lu-systems.

Crystals in the optimal oxygen-saturated state have high superconducting transition parameters, $T_c=90$ - 92 K , $\Delta T_c=0.2$ - 0.5 K . X-ray powder patterns from 123-Lu crystals in the as-grown state show a typical picture for the orthorhombic 123-R structure (Fig. 5a). But crystals obtained at high rates of cooling (10 - 20 K/hour) had a tetragonal structure (Fig. 5b); and it is these crystals which have been studied by X-ray single crystal diffraction method.

The crystal data are: tetragonal, space group P4/

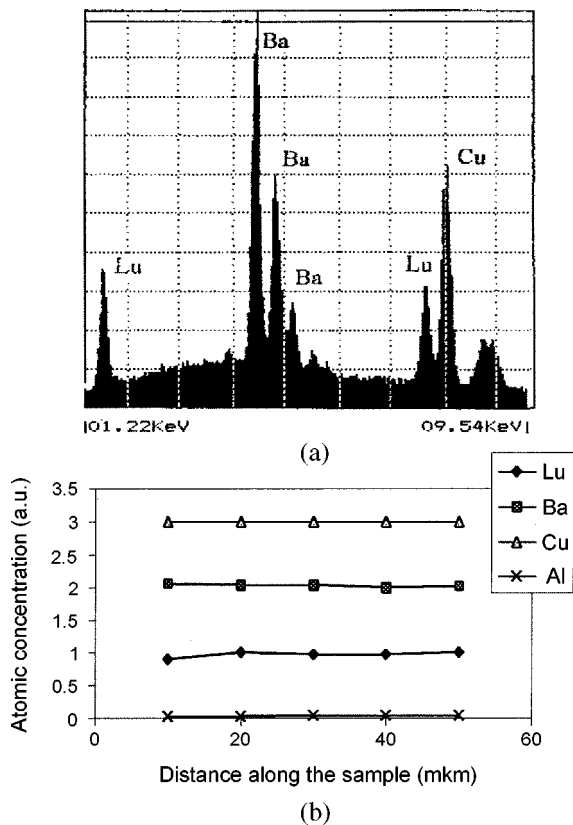


Fig. 4. EDX analysis (a) and elemental profiles (b) along 123-Lu crystal.

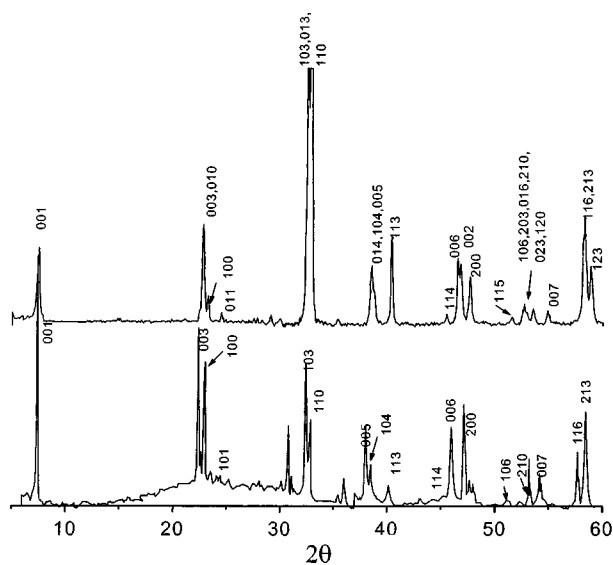


Fig. 5. XRD patterns of ground 123-Lu crystals: orthorhombic phase, $a=3.822$, $b=3.883$, $c=11.69$ Å (a) and tetragonal phase $a=3.846$, $c=11.845$ Å (b). Peaks for orthorhombic phase were indexed by comparing with literature data [23] for orthorhombic 123-Tm. Peaks for the tetragonal phase were calculated from our experimental data.

mmm , $a=3.8404(5)$ Å, $c=11.818(3)$ Å, $V=174.30(5)$ Å³, $Z=1$, $D_x=7.014$ g/cm³, MoK α radiation, $\lambda=0.71073$ Å, cell parameters from 24 reflections (with Fridel),

Table 2. Fractional atomic coordinates ($\times 10^4$), equivalent isotropic ($\times 10^3$) and anisotropic displacement parameters (Å² $\times 10^3$) for $T=\exp[-2\pi^2\{h^2a^*2U_{11}+\dots+2hka^*b^*U_{12}\}]$, $U_{ij}=0$ if $i\neq j$

Atom	x	y	z	U_{eq}	U_{11}	U_{22}	U_{33}
Lu	5000	5000	5000	6(1)	5(1)	5(1)	8(1)
Ba	5000	5000	1958(1)	9(1)	8(1)	8(1)	11(1)
Cu1	0	0	0	12(3)	11(1)	11(1)	13(1)
Cu2	0	0	3635(1)	7(1)	4(1)	4(1)	13(1)
O1	0	0	1526(5)	13(1)	15(1)	15(1)	11(1)
O2	0	5000	3813(4)	9(1)	9(1)	4(1)	12(1)

$\theta=10-15^\circ$, $\mu=34.099$ mm⁻¹, crystal size (0.51 \times 0.32 \times 0.014 mm) and with the habit shown in Fig. 6.

The data collection were: $\omega-2\theta$, $\theta_{max}=35^\circ$, absorption correction analytical, $T_{min}=0.0351$, $T_{max}=0.6185$, 1712 measured reflections, 288 independent reflections, 279 observed reflections [$I_{hkl}>2\sigma(I)$], $R_{int}=0.036$, three control reflections, intensity decay < 4%.

The basis of refinement was: refinement on F^2 , SHELX97 [24], $R_1=0.0240$, $wR_2=0.0549$ for 249 observed reflections and $R_1=0.0246$ and $wR_2=0.0552$ for 288 independent reflections. The initial coordinates of atoms for the structural refinement have been used from [25] for 123-Y. The fractional atomic coordinates, equivalent isotropic and anisotropic displacement parameters are given in Table 2. Refinement of the site occupation factor (s.o.f.) was carried out for all atoms. It was shown that these parameters are identical to those for space group $P4/mmm$ in the "International Tables for Crystallography". The difference in electron density at $x=0.5$, $y=0$, $z=0$ has shown that there are no atoms in this position. Consequently, the composition of the crystal studied must correspond to $LuBa_2Cu_3O_6$, i.e. with $x=0$.

The environment of each metal atom is typical for 123-R compounds: dumb-bells and pyramids for Cu(1)

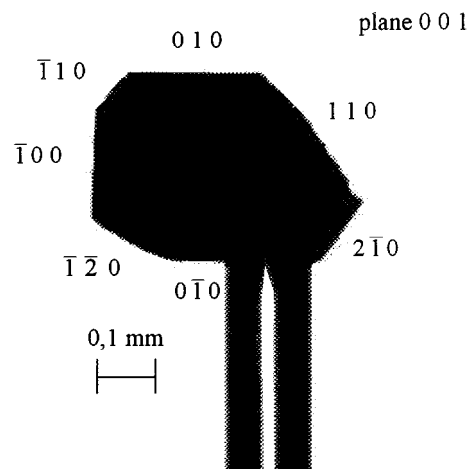


Fig. 6. Micrograph and faces of crystal. Distances from crystal center to planes (0 1 0), (1 1 0), (2 1 0), (0 1 0), ($\bar{1}$ 2 0), ($\bar{1}$ 0 0), (1 0 0), (0 0 1), (0 0 $\bar{1}$) are 0.164, 0.157, 0.270, 0.164, 0.186, 0.236, 0.229, 0.007, 0.007 mm

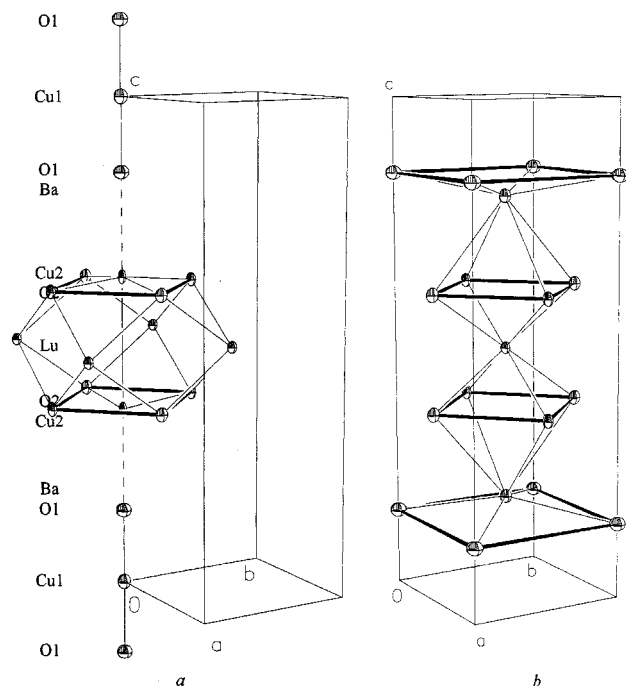


Fig. 7. Environment of cations Cu (a) and Lu, Ba- (b) by anions. Bold lines shows layers formed by oxygen atoms.

Table 3. Selected interatomic distances d (Å)

Bond	d , Å	Bond	d , Å
Lu-O2	2.378(3)×8	Lu···Cu2	3.1585(7)×4
Ba-O1	2.763(1)×4	Ba···Cu2	3.3623(8)×4
Ba-O2	2.914(4)×4	Ba···Cu1	3.5673(5)×4
Cu1-O1	1.803(6)×2	Cu2···Cu2 ⁱ	3.226(1)
Cu2-O1	2.493(6)	Ba···Lu	3.596(1)
Cu2-O2	1.9316(6)×4		

and Cu(2) respectively; a non-uniform antiprism for Ba and a cube for Lu (Fig. 7). Selected interatomic distances are presented in Table 3; the shortest distances between metal atoms can be found here. The Cu environment and the values of interatomic distances indicate that the oxidation states of Cu atoms are 1+ and 2+; this is in a good agreement with the stoichiometry of the crystals.

Conclusions

We firstly prepared large single crystals of $\text{LuBa}_2\text{Cu}_3\text{O}_{6+x}$ based on optimal growing conditions and the melting temperature of this phase. The crystal structure was solved by an X-ray diffraction method. The conclusions were made as following: the difficulties in preparation of the $\text{LuBa}_2\text{Cu}_3\text{O}_{6+x}$ phase are not due to steric factors (the smallest ion Lu among

rare earth elements) but some technological parameters, mainly the very narrow interval of its thermal stability.

The work was supported by grant N 00-02-17914 from RFBR, grant N 98009 from the State scientific program on physics of condensed matter (section "Superconductivity").

References

1. P.H. Hor, R.L. Meng, Y.G. Wang, L. Gao, Z.J. Huang, J. Bechtold, K. Forster, and C.W. Chu, *Phys. Rev. Lett.* 58[18] (1987) 1891-1894.
2. J.M. Tarascon, W.R. McKinnon, L.H. Green, G.W. Hull, and E.M. Vogel, *Phys. Rev. B.* 36[1] (1987) 226-234.
3. S. Ramesh and M.S. Hegde, *Physica C* 230[1] (1994) 135-140.
4. E. Hodorowicz, S.A. Hodorowicz, and H.A. Eick, *J. Alloys Compounds* 181 (1992) 445-455.
5. C. Andreouli and A. Tsetsekou, *Physica C* 291 (1997) 274-286.
6. X. Chen, Y. Quan, Z. Chen, and G. Zhou, *Phys. Stat. Sol.(a)* 130 (1992) 415-420.
7. Y. Xu and W. Guan, *Physica C* 212 (1993) 119-127.
8. M. Murakami, N. Sakai, T. Higuchi, and S.I. Yoo, *Superconductor Sci. Technol.* 9[12] (1996) 1015-1018.
9. A.N. Lavrov and L.P. Kozeeva, *Russ. Inorg. Materials, Eng. Trans.* 34[11] (1998) 1177-1185.
10. T. Itoh, M. Uzawa, and H. Uchikawa, *J. Crystal Growth* 91 (1988) 397-401.
11. P. Somasurandaram, A. Mohan Ram, A.M. Umarji, and C.N.R. Rao, *Mater. Res. Bull.* 25 (1990) 331-335.
12. B. Zhou, I. Buan, S.W. Pierson, C.C. Huang, and O.T. Valls, *Phys. Rev. B* 47[17] (1993) 11631-11634.
13. I.Buan, O. Bronk, P. Stojkovic, and N.E. Israeloff, A.M. Goldman, C.C. Huang, O.T. Valls, I.Z. Liu, and R. Shelton, *Phys. Rev. Lett.* 72[16] (1994) 2632-2635.
14. I.Buan, B. Zhou, C.C. Huang, I.Z. Liu, and R. Shelton, *Phys. Rev. B* 49[17] (1994) 12220-12223.
15. L.P. Kozeeva, L.I. Yudanova, and A.N. Lavrov, *Russ. J. Inorg. Chem.* 41[9] (1996) 1413-1415.
16. L.P. Kozeeva, M.Yu. Kameneva, A.N. Lavrov, and E.V. Sokol, *Russ. Inorganic Materials, Eng. Trans.* 34[10] (1998) 1057-1064.
17. A.N. Lavrov and L.P. Kozeeva, *Physica C* 248 (1995) 365-381.
18. E.A. Gudilin, N.N. Oleinikov, and Yu.D. Tretyakov, *Russ. J. Inorg. Chem.* 41[6] (1996) 887-898.
19. V.K. Yanovskii, Z.I. Voronkova, I.V. Vodolazskaya, I.N. Leontieva, and T.P. Petrovskaya, *Russ. Supercond. Phys. Chem. Techn.* 2[3] (1989) 30-33.
20. K. Akinori, H. Yoshikazu, and O. Hideaki, *Jap. J. Appl. Phys.* 26[9] (1987) L1521-1523.
21. K. Lee, B.K. Leon, G. Park, P. Song, and S.P. Choi, *Solid State Commun.* 79[3] (1991) 237-240.
22. J. Wojcik, M. Rosochovska, H. Niculescu, and A. Pajaczowska, *J. Crystal Growth* 91 (1988) 255-260.
23. E. Hodorowicz, S.A. Hodorowicz, and H.A. Eick, *Physica C*, 158 (1989) 127-136.
24. G.M. Sheldrick, *SHELX97*, release 97-2, University of Göttingen, Germany, 1997.
25. W-J. Jang, H. Mori, M. Watahiki, S. Tajima, N. Koshizuka, and S. Tanaka, *J. Solid State Chem.* 130 (1997) 42-47.